Preprints of the 19th World Congress
The International Federation of Automatic Control
Cape Town, South Africa. August 24-29, 2014

$\mathcal{H}_\infty$-Controller Design Methods Applied to One Joint of a Flexible Industrial Manipulator ⋆

Patrik Axelsson, * **Anders Helmersson,** * **Mikael Norrlöf** *,**

* *Division of Automatic Control, Department of Electrical Engineering, Linköping University, SE-581 83 Linköping, Sweden (e-mail: {axelsson, andersh, mino}@isy.liu.se).*
** *ABB AB – Robotics SE-721 68 Västerås, Sweden*

Abstract: Control of a flexible joint of an industrial manipulator using $\mathcal{H}_\infty$ design methods is presented. The considered design methods are i) mixed-$\mathcal{H}_\infty$ design, and ii) $\mathcal{H}_\infty$ loop shaping design. Two different controller configurations are examined: one uses only the actuator position, while the other uses the actuator position and the acceleration of the end-effector. The four resulting controllers are compared to a standard PID controller where only the actuator position is measured. The choices of the weighting functions are discussed in details. For the loop shaping design method, the acceleration measurement is required to improve the performance compared to the PID controller. For the mixed-$\mathcal{H}_\infty$ method it is enough to have only the actuator position to get an improved performance. Model order reduction of the controllers is briefly discussed, which is important for implementation of the controllers in the robot control system.

Keywords: Robotics, Flexible, H-infinity control, Accelerometers

1. INTRODUCTION

The requirements for controllers in modern industrial manipulators are that they should provide high performance, at the same time, robustness to model uncertainty. In the typical standard control configuration the actuator positions are the only measurements used in the higher level control loop. At a lower level, in the drive system, the currents and voltages in the motor are measured to provide torque control for the motors. In this contribution different $\mathcal{H}_\infty$-controller design schemes are compared when using two different sensor configurations. First, the standard case where only the position of the actuator rotation is used, and second a configuration where, in addition, the acceleration of the tool tip is measured. Two different $\mathcal{H}_\infty$ methods are investigated: i) loop shaping [McFarlane and Glover, 1992], and ii) multi-$\mathcal{H}_\infty$ design [`mixedHinfsyn`, 2013, Zavari et al., 2012].

Motivated by the conclusions from Sage et al. [1999] regarding the area of robust control applied to industrial manipulators, this contribution includes:

- results presented using realistic models,
- a comparison with a standard PID control structure,
- model reduction of the controllers to get a result that more easily can be implemented in practice.

The model used in this contribution represents one joint of a typical modern industrial robot [Moberg et al., 2009]. It is a physical model consisting of four masses, which should be compared to the typical two-mass model used in many previous contributions, see Sage et al. [1999] and the references therein. The joint model represents the first joint of a serial 6-DOF industrial manipulator, where the remaining five axes have been configured to minimise the couplings to the first axis. To handle changes in the configuration of the remaining axes, gain scheduling techniques can be used based on the results in this paper.

An important part of the design is the choice of the weighting functions, which is an essential task to get a satisfactory performance. The work of choosing the weights is difficult, tedious and time consuming. This can be be the reasons for why $\mathcal{H}_\infty$ methods are not used that often in practice even though the performance and robustness can be increased. In particular, the use of two measurements for control of one variable requires special treatment. The development of the weighting functions for the four controllers are discussed in details, and provides a significant part of the contributions in the paper.

Controller synthesis using $\mathcal{H}_\infty$ methods has been proposed in Song et al. [1992], Stout and Sawan [1992], where the complete non-linear robot model first is linearised using exact linearisation, second an $\mathcal{H}_\infty$ controller is designed using the linearised model. The remaining non-linearities due to model errors are seen as uncertainties and/or disturbances. In both papers, the model is rigid and the $\mathcal{H}_\infty$ controller, using only joint positions, is designed using the mixed-sensitivity method. In Sage et al. [1997] $\mathcal{H}_\infty$ loop shaping with measurements of the actuator positions is applied to a robot. The authors use a flexible joint model which has been linearised. The linearised model makes it possible to use decentralised control, hence $\mathcal{H}_\infty$ loop shaping is applied to n SISO-systems instead of the complete MIMO-system.

⋆ This work was supported by the Vinnova Excellence Center LINK-SIC and by the Excellence Center at Linköping-Lund in Information Technology, ELLIIT.

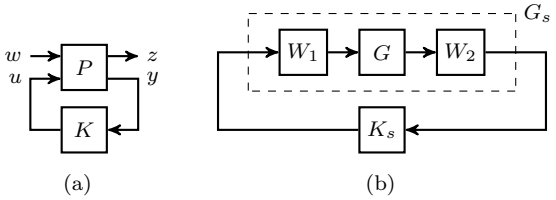

Fig. 1. System description for general $\mathcal{H}_\infty$ synthesis (a) and loop shaping (b).

Explicit use of acceleration measurements for control in robotic applications has been reported in, for example, de Jager [1993], Dumetz et al. [2006], Kosuge et al. [1989], Readman and Bélanger [1991] and Xu and Han [2000]. In Dumetz et al. [2006], a control law using motor position and acceleration of the load in the feedback loop is proposed for a Cartesian robot [1] . The robot is assumed to be flexible and modelled as a two-mass system, where the masses are connected by a linear spring-damper pair. Another control law of a Cartesian robot using acceleration measurements is presented in de Jager [1993]. The model is a rigid joint model and the evaluation is made both in simulation and experiments.

In Kosuge et al. [1989] a 2-*degree-of-freedom* (DOF) manipulator is controlled using acceleration measurements of the end-effector. The model is assumed to be rigid and it is exactly linearised. The joint angular acceleration used in the non-linear feedback loop is calculated using the inverse kinematic acceleration model and the measured acceleration. The use of direct measurements of the angular acceleration in the feedback loop is presented in Readman and Bélanger [1991] for both rigid and flexible joint models. A more recent work is presented in Xu and Han [2000], where a 3-DOF manipulator is controlled using only measurements of the end-effector acceleration.

The theory for synthesis of $\mathcal{H}_\infty$ controllers is presented in Section 2. The model describing the robot joint is explained in Section 3. In Section 4, the requirements of the system as well as the design of four controllers are described, and in Section 5 the simulation results are shown. Finally, Section 6 discuss low order controller synthesis and Section 7 concludes the work.

2. CONTROLLER DESIGN METHODS

In this section, a brief introduction to mixed-$\mathcal{H}_\infty$ design [`mixedHinfsyn`, 2013, Zavari et al., 2012] and $\mathcal{H}_\infty$ loop shaping [McFarlane and Glover, 1992] will be presented.

2.1 Mixed-$\mathcal{H}_\infty$ Controller Design

A common design method is to construct the system $P(s)$ in

$$\begin{pmatrix} z \\ y \end{pmatrix} = \begin{pmatrix} P_{11}(s) & P_{12}(s) \\ P_{21}(s) & P_{22}(s) \end{pmatrix} \begin{pmatrix} w \\ u \end{pmatrix} = P(s) \begin{pmatrix} w \\ u \end{pmatrix} \tag{1}$$

by augmenting the original system $y = G(s)u$ with the weights $W_u(s)$, $W_S(s)$, and $W_T(s)$, such that the system $z = F_l(P, K)w$, depicted in Figure 1(a), can be written as

[1] For a Cartesian robot the joint acceleration is measured directly by an accelerometer, while for a serial type robot there is a non-linear mapping depending on the states.

$$F_l(P, K) = \begin{pmatrix} W_u(s)G_{wu}(s) \\ -W_T(s)T(s) \\ W_S(s)S(s) \end{pmatrix}, \tag{2}$$

where $S(s) = (I + G(s)K(s))^{-1}$ is the sensitivity function, $T(s) = I - S(s)$ is the complementary sensitivity function, and $G_{wu}(s) = -K(s)(I + G(s)K(s))^{-1}$ is the transfer function from w to u. The $\mathcal{H}_\infty$-controller is then obtained by minimising the $\mathcal{H}_\infty$-norm of the system $F_l(P, K)$, i.e., minimise γ such that $\|F_l(P, K)\|_\infty < \gamma$. Using (2) gives

$$|W_u(i\omega)G_{wu}(i\omega)| < \gamma, \ \forall\omega, \tag{3a}$$
$$|W_T(i\omega)T(i\omega)| < \gamma, \ \forall\omega, \tag{3b}$$
$$|W_S(i\omega)S(i\omega)| < \gamma, \ \forall\omega. \tag{3c}$$

The transfer functions $G_{wu}(s)$, $S(s)$, and $T(s)$ can now be shaped to satisfy the requirements by choosing the weights $W_u(s)$, $W_S(s)$, and $W_T(s)$. The aim is to get a value of γ close to 1, which in general is a hard to achieve and it requires insight in the deign method as well as the system dynamics. For more details about the design method, see e.g. Skogestad and Postletwaite [2005], Zhou et al. [1996].

The mixed-$\mathcal{H}_\infty$ controller design [`mixedHinfsyn`, 2013, Zavari et al., 2012] is a modification of the standard $\mathcal{H}_\infty$ design method. Instead of choosing the weights in (2) such that the norm of all weighted transfer functions satisfies (3), the modified method divides the problem into design constraints and design objectives. The controller can now be found as the solution to

$$\underset{K(s)}{\text{Minimise}} \quad \gamma \tag{4a}$$
$$\text{subject to} \quad \|W_P(s)S(s)\|_\infty < \gamma \tag{4b}$$
$$\|M_S(s)S(s)\|_\infty < 1 \tag{4c}$$
$$\|W_u(s)G_{wu}(s)\|_\infty < 1 \tag{4d}$$
$$\|W_T(s)T(s)\|_\infty < 1 \tag{4e}$$

where γ not necessarily has to be close to 1. Here, the weight $W_S(s)$ has been replaced by the weights $M_S(s)$ and $W_P(s)$. The method can be generalised to other control structures and in its general form it is formulated as a multi-objective optimisation problem. More details about the general form and how to solve the optimisation problem are presented in `mixedHinfsyn` [2013], Zavari et al. [2012].

2.2 Loop Shaping using $\mathcal{H}_\infty$ Synthesis

For loop shaping [McFarlane and Glover, 1992], the system $G(s)$ is pre- and post-multiplied with weights $W_1(s)$ and $W_2(s)$, see Figure 1(b), such that the shaped system $G_s(s) = W_2(s)G(s)W_1(s)$ has the desired properties. The controller $K_s(s)$ is then obtained using the method described in Glover and McFarlane [1989] applied on the system $G_s(s)$, giving the controller $K_s(s)$. Finally, the controller $K(s)$ is given by

$$K(s) = W_1(s)K_s(s)W_2(s). \tag{5}$$

Note that the structure in Figure 1(b) for loop shaping can be rewritten as a standard $\mathcal{H}_\infty$ problem according to Figure 1(a), see Zhou et al. [1996] for details. It will be used in Section 6 for synthesis of low order controllers.

The MATLAB function `ncfsyn`, included in the Robust Control Toolbox, is used in this paper for synthesis of $\mathcal{H}_\infty$ controllers using loop shaping.

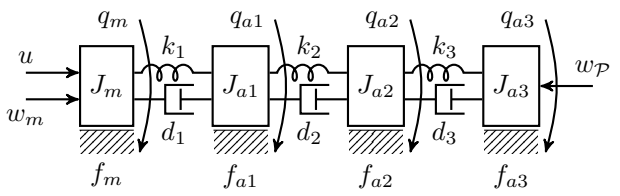

Fig. 2. A four-mass flexible joint model, where J_m is the motor inertia and J_{a1}, J_{a2}, and J_{a3} are the distributed arm inertias.

3. FLEXIBLE JOINT MODEL

The model considered in this paper is a four-mass benchmark model of a single flexible joint, see Figure 2, presented in Moberg et al. [2009]. The model corresponds to joint 1 of a serial 6-DOF industrial manipulator, where the five remaining axes are configured such that the couplings to joint 1 is minimised, see Moberg et al. [2009] for more details about the operating point where the model has been linearised.

Input to the system is the motor torque u, the motor disturbance w_m and the end-effector disturbance $w_{\mathcal{P}}$. The four masses are connected by spring-damper pairs, where the first mass corresponds to the motor. The other masses represents distributed masses placed along the arm. The first spring-damper pair is modelled by a linear damper and non-linear spring, whereas the other spring-damper pairs are modelled as linear springs and dampers. The non-linear spring is characterised by a low stiffness for low deflections and a high stiffness for high deflections. This behaviour is typical for compact gear boxes, such as harmonic drive [Ruderman and Bertram, 2012]. For design of the $\mathcal{H}_\infty$ controllers, the non-linear model is linearised in one operating point in the high stiffness region, motivated by that a constant torque, e.g. gravity, is acting on the joint. Moreover, the friction torques are assumed to be linear and the input torque u is limited to $\pm 20\,\text{Nm}$. The output of the system is the motor position q_m and the end-effector acceleration $\ddot{\mathcal{P}}$, where

$$\mathcal{P} = \frac{l_1 q_{a1} + l_2 q_{a2} + l_3 q_{a3}}{\eta}. \tag{6}$$

In (6), η is the gear ratio and l_1, l_2, and l_3 are the respective link lengths.

Using Lagrange's equation, the linearised flexible joint model can be described by a set of four ODEs, which can be reformulated as a linear state space model according to

$$\dot{x} = Ax + Bu + B_w w, \tag{7a}$$
$$y = Cx + Du + D_w w. \tag{7b}$$

where the state vector and disturbance vector are given by

$$x = (q_m \;\; q_{a1} \;\; q_{a2} \;\; q_{a3} \;\; \dot{q}_m \;\; \dot{q}_{a1} \;\; \dot{q}_{a2} \;\; \dot{q}_{a3})^\mathsf{T}, \tag{8a}$$
$$w = (w_m \;\; w_{\mathcal{P}})^\mathsf{T}. \tag{8b}$$

The linear state space model is used for design of the $\mathcal{H}_\infty$ controllers. Note that the matrices C, D, and D_w are different depending on which sensor configuration that is used, whereas the matrices A, B, and B_w stay the same.

4. DESIGN OF CONTROLLERS

In this section, four controllers based on the methods in Sections 2.1 and 2.2 are considered, using only the motor angle q_m or both q_m and the acceleration of the end-effector $\ddot{\mathcal{P}}$. The controllers are

(1) $\mathcal{H}_\infty^{ls}(q_m)$: Loop shaping controller using q_m.
(2) $\mathcal{H}_\infty^{ls}(q_m, \ddot{\mathcal{P}})$: Loop shaping controller using q_m and $\ddot{\mathcal{P}}$.
(3) $\mathcal{H}_\infty^{m}(q_m)$: Mixed-$\mathcal{H}_\infty$ controller using q_m.
(4) $\mathcal{H}_\infty^{m}(q_m, \ddot{\mathcal{P}})$: Mixed-$\mathcal{H}_\infty$ controller using q_m and $\ddot{\mathcal{P}}$.

The four controllers are compared to a PID controller where only q_m is used. The PID controller is tuned to give the same performance as the best controller presented in Moberg et al. [2009].

To get high enough gain for low frequencies, without having the pole exactly in 0, the break-point of the magnitude function has to be very small, around $10^{-5}\,\text{rad/s}$. From Figure 3 it can be seen that the main dynamics of the system is present in the frequency interval 30-110 rad/s. The large frequency span from $10^{-5}\,\text{rad/s}$ to $110\,\text{rad/s}$ makes it numerically difficult to solve for the controller using the standard iterative methods described in Skogestad and Postletwaite [2005], Zhou et al. [1996]. The mixed-$\mathcal{H}_\infty$ method does not suffer from this, since the design objectives (choice of W_P) for low frequencies is separated from the design constraints (choice of M_S).

4.1 Requirements

The controllers using $\mathcal{H}_\infty$ methods are designed to give better performance than the PID controller. In practice it means that the $\mathcal{H}_\infty$ controllers should attenuate the disturbances at least as much as the PID controller and the cut-off frequency should be approximately the same.

In Figure 3, the singular values of the systems from w to $y = q_m$ and w to $y = \begin{pmatrix} q_m & \ddot{\mathcal{P}} \end{pmatrix}^\mathsf{T}$ show that an integrator is present. It means that in order to attenuate piecewise constant disturbances, it is required to have at least two integrators in the open loop GK. Since G already has one integrator, the other integrators have to be included in the controller K. For controllers 2 and 4, an integrator will be present if W_1 or W_2 include an integrator, recall (5). The requirements for controllers 1 and 3 become that $|S(i\omega)| \to 0$ for $\omega \to 0$. Note that it is not possible to stabilise the plant $P(s)$ with marginally stable weights. Instead the pole has to be moved into the left half plan a small distance.

4.2 Choice of Weights

4.2.1. $\mathcal{H}_\infty^{ls}(q_m)$: Using only q_m as a measurement gives a SISO-system, hence W_1 and W_2 are scalar transfer functions. For a linear SISO-system it is possible to use one of W_1 and W_2 since the transfer functions commute with the system $G(s)$. Therefore, $W_1(s) = 1$ and $W_2(s)$ is chosen such that the desired loop shape is obtained. First of all, it is necessary to have an integrator as discussed above. Having a pure integrator will lead to that the phase margin will be decreased, a zero in $s = -10$ is therefore added in order not to change the loop gain for frequencies above 10 rad/s. Next, the gain is increased to get the desired cut-off frequency. The result using the weight is that the loop shape have peaks above 30 rad/s. To reduce

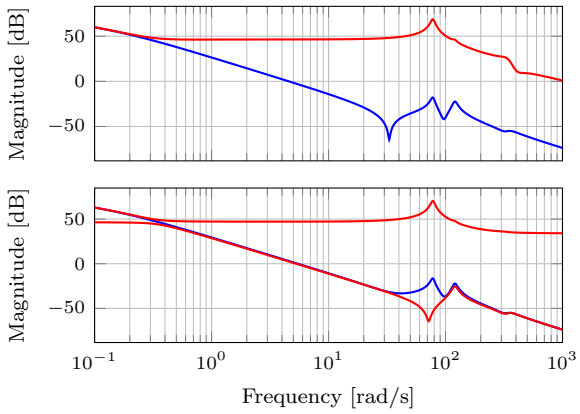

Fig. 3. Singular values for the system from u to y (top) and w to y (bottom), for $y = q_m$ (blue) and $y = (q_m \;\; \ddot{\mathcal{P}})^\mathsf{T}$ (red).

the magnitude of the peaks a modified elliptic filter [2]

$$H(s) = \frac{0.5227s^2 + 3.266s + 1406}{s^2 + 5.808s + 2324} \tag{9}$$

is introduced in W_2. The weights are finally given as

$$W_1(s) = 1, \quad W_2(s) = 100\frac{s+10}{s}H(s). \tag{10}$$

Using `ncfsyn` a controller of order 13 is obtained.

4.2.2. $\mathcal{H}_\infty^{ls}(q_m, \ddot{\mathcal{P}})$: Adding an extra measurement signal in terms of the acceleration of the end-effector gives a system with one input and two outputs. For stability reasons, it is not possible to have an integrator in both control channels. Therefore, the integrator is placed in the channel for q_m since the accelerometer measurement has low frequency noise, such as drift. For the same reason as for the other controller, a zero in $s = -3$ is introduced. The transfer function from input torque to acceleration of the end-effector has a high gain in the frequency range of interest. To decrease the gain such that it is comparable with the motor angle measurement, a low pass filter is added in the acceleration channel. The final weights are

$$W_1(s) = 50, \quad W_2(s) = \text{diag}\left(\frac{s+3}{s}, \frac{0.2}{(s+5)^2}\right), \tag{11}$$

giving a controller of order 13. Introducing an elliptic filter to attenuate the peaks in the open loop did not give the same results as for the $\mathcal{H}_\infty^{ls}(q_m)$-controller. Instead of improving the loop gain, the elliptic filter made it worse.

4.2.3. $\mathcal{H}_\infty^{m}(q_m)$: For this controller, four different weights have to be chosen, recall (4). The weight M_S should limit the peak of S and is therefore chosen to be a constant [3]. The peak of G_{wu} is also important to reduce in order to keep the control signal bounded, especially for high frequencies. A constant value of W_u is therefore also chosen. In the spirit of try simplest thing first, the weight W_T is also chosen to be a constant

In order to attenuate the disturbances it is, as was mentioned above, necessary to have at least one integrator in the controller. Forcing S to 0 is the same as letting W_P approach ∞ when $\omega \to 0$. To get a proper inverse, a zero is also included in the weight. Since a pure integrator is not used, the slope of the weight has to be higher than 20 dB per decade frequency, in order to force S to be low enough. This was accomplished by taking the weight to the power of 3 (2 was not enough). The numerical values of the weights are chosen as

$$W_u = 10^{-50/20}, \quad W_T = 10^{-10/20}, \tag{12a}$$

$$M_S = 10^{-10/20}, \quad W_P = \left(\frac{s+100.1}{s+0.1}\right)^3. \tag{12b}$$

The constant weights in the form $10^{-\alpha/20}$ can be interpret as a maximum value, for the corresponding transfer function, of α dB. The resulting controller is of order 10.

4.2.4. $\mathcal{H}_\infty^{m}(q_m, \ddot{\mathcal{P}})$: Like for the controller $\mathcal{H}_\infty^{ls}(q_m, \ddot{\mathcal{P}})$, designing the weights for the mixed-$\mathcal{H}_\infty$ method becomes somewhat more involved with two measurements and one control signal. The aim is to attenuate the disturbances influence on the end-effector position. A variant is to find a rough estimate of the end-effector position and then choosing the weights from that. A straightforward estimate of $\mathcal{P}$ using $\ddot{\mathcal{P}}$ is

$$\hat{\mathcal{P}} = \frac{1}{s^2}\ddot{\mathcal{P}}. \tag{13}$$

Due to low frequency drift and bias in an accelerometer, this estimate is only useful for high frequencies. A high pass filter is therefore used according to

$$\hat{\mathcal{P}}_{\text{high}} = c_2\frac{s^2}{(p+s)^2}\frac{1}{s^2}\ddot{\mathcal{P}} = c_2\frac{1}{(p+s)^2}\ddot{\mathcal{P}} \tag{14}$$

where c_2 and p are constants to choose. Another straightforward estimate of $\mathcal{P}$ is to use the motor angle q_m according to $\hat{\mathcal{P}} = lq_m$ where l is the length of the arm. Compared to the estimated position using the acceleration, this new estimate is only valid for low frequencies. Using a low pass filter gives an estimate for low frequencies. It is important that the two estimates do not overlap each other, hence the low pass filter is chosen as the complementarity to the previous used high pass filter. The low frequency estimate is now given by

$$\hat{\mathcal{P}}_{\text{low}} = c_1\left(1 - \frac{s^2}{(p+s)^2}\right)lq_m = c_1\frac{2s+p}{(p+s)^2}plq_m \tag{15}$$

where c_1 is a design variable. The final estimate of $\mathcal{P}$ is the sum of the two estimates above, hence

$$\hat{\mathcal{P}} = \underbrace{\begin{pmatrix} c_1\frac{2s+p}{(p+s)^2}pl & c_2\frac{1}{(p+s)^2}\end{pmatrix}}_{W}\begin{pmatrix} q_m \\ \ddot{\mathcal{P}}\end{pmatrix} \tag{16}$$

Using the weights

$$M_S = \tilde{M}_S W, \quad W_P = \tilde{W}_P W, \quad W_T = \tilde{W}_T W, \tag{17}$$

where $\tilde{M}_S$, $\tilde{W}_P$, and $\tilde{W}_T$ can be designed in a similar way as in Section 4.2.3, makes it possible to use more than one output together with one input. The last weight W_u can be chosen similar as in Section 4.2.3. The numerical values of the weights are

$$W_u = 10^{-40/20}, \quad W = \begin{pmatrix}\frac{30s+75}{(s+5)^2} & \frac{0.1}{(s+5)^2}\end{pmatrix}, \tag{18a}$$

$$\tilde{M}_S = 10^{-2/20}, \quad \tilde{W}_P = \left(\frac{s+80}{s+0.15}\right)^3. \tag{18b}$$

[2] The filter is designed to have a magnitude of 0 dB up to 50 rad/s, after that -10 dB, but due to ripple, the real magnitude will differ from that.

[3] More complicated weights can be used but here we try simple things first.

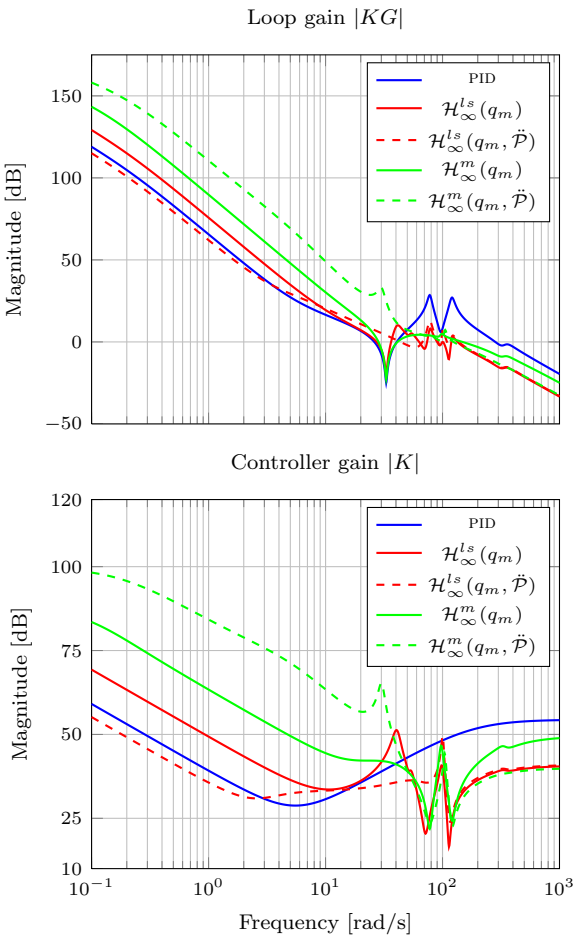

Fig. 4. Loop gain $|KG|$ and controller gain $|K|$ for the five controllers.

and it turns out that W_T is not needed for the performance. Using these weights results in a controller of order 13.

4.3 Controller Characteristics

The resulting loop gain for the five controllers are shown in Figure 4. The four controllers using $\mathcal{H}_\infty$-methods do not give as high peaks as the PID-controller around 100 rad/s. It can also be seen that introducing $\ddot{\mathcal{P}}$ as a measurement eliminates the notch at 30 rad/s.

In Figure 4, the magnitude of the five controllers are presented. The PID controller is smoother than the other controllers. The reason is that a part of the system dynamics is included in the $\mathcal{H}_\infty$-controllers. As a result, they try to remove the resonance peaks from the system, which can be seen in Figure 3, hence the peaks in the amplitude function of the $\mathcal{H}_\infty$-controllers. The weights W_u for the controllers $\mathcal{H}_\infty^m(q_m)$ and $\mathcal{H}_\infty^m(q_m, \ddot{\mathcal{P}})$ are different which can be seen in Figure 4 for high frequencies. Comparing the two controllers $\mathcal{H}_\infty^{ls}(q_m)$ and $\mathcal{H}_\infty^{ls}(q_m, \ddot{\mathcal{P}})$ for high frequencies it can be seen that they behave similar. The PID-controller has the highest magnitude for high frequencies, which implies that the measurement noise will be amplified more than for the $\mathcal{H}_\infty$-controllers.

5. SIMULATION RESULTS

The five controllers are evaluated using a simulation model. The simulation model consists of the flexible joint model described in Section 3, a measurement system, and a controller. The robot joint model is implemented in continuous time whereas the controllers operate in discrete time. The continuous-time controllers developed in Section 4, are therefore discretized using Tustin's formula. The measurements are affected by a time delay of one sample as well as zero mean normal distributed measurement noise. The sample time is $T_s = 0.5$ ms.

The system is excited by a disturbance signal w containing steps and chirp signals on both the motor and end-effector. The performance is evaluated using a performance index, which is a weighted sum of peak-to-peak errors and settling times in the simulated end-effector position and the maximum torque and the torque noise in the simulated motor torque. The reader is referred to Moberg et al. [2009] for complete details about the disturbance signals and the performance index.

Figure 5 shows how the motor torque differs between the five controllers. In the upper diagram it can be see that $\mathcal{H}_\infty^{ls}(q_m)$ gives higher torques than the PID and the $\mathcal{H}_\infty^m(q_m)$ controllers. The PID gives higher torque noise during steady state due to the gain of the controller for high frequencies, recall Figure 4. In the lower diagram in Figure 5 it is shown that the controllers $\mathcal{H}_\infty^{ls}(q_m, \ddot{\mathcal{P}})$ and $\mathcal{H}_\infty^m(q_m, \ddot{\mathcal{P}})$ give similar torque signals, and lower compared to the PID controller. A low torque signal is preferred to reduce the energy consumption and to decrease the wear in the motor and gear.

The end-effector position is presented in Figure 6. In the top graph it is seen that $\mathcal{H}_\infty^{ls}(q_m)$ gives, compared to the PID, higher oscillations during the time intervals 10-15 s and 37-42 s, which corresponds to a chirp disturbance at the end-effector. For step disturbances and chirp disturbances on the motor (time intervals 16-21 s and 43-58 s) $\mathcal{H}_\infty^{ls}(q_m)$ and the PID are more similar. The controller $\mathcal{H}_\infty^m(q_m)$ is better than the other two controllers in the simulation. The bottom graph shows that $\mathcal{H}_\infty^m(q_m, \ddot{\mathcal{P}})$ can handle the chirp disturbances on the motor (time intervals 16-21 s and 43-58 s) and step disturbances very good. For a chirp disturbance on the end-effector, the two $\mathcal{H}_\infty$ controllers give similar results. For step disturbances, the controller $\mathcal{H}_\infty^{ls}(q_m, \ddot{\mathcal{P}})$ gives lower peaks than the PID controller, however the settling time is longer. The steady state error of approximately 2 mm after 25 s is a result of a constant torque disturbance on the end-effector. The size of the error will depend on the size of the disturbance and the stiffness of the joint. The motor position, which is measured, is controlled to zero for all five controllers.

The performance index for the five controllers is presented in Table 1. It shows, as discussed above, that $\mathcal{H}_\infty^{ls}(q_m)$ and the PID controller behave similar and that $\mathcal{H}_\infty^{ls}(q_m, \ddot{\mathcal{P}})$ and $\mathcal{H}_\infty^m(q_m)$ give similar behaviour. The $\mathcal{H}_\infty^m(q_m, \ddot{\mathcal{P}})$-controller gives the best result.

6. LOW ORDER SYNTHESIS

For implementation of the controller in the robot control system it is important to have a low order controller. A

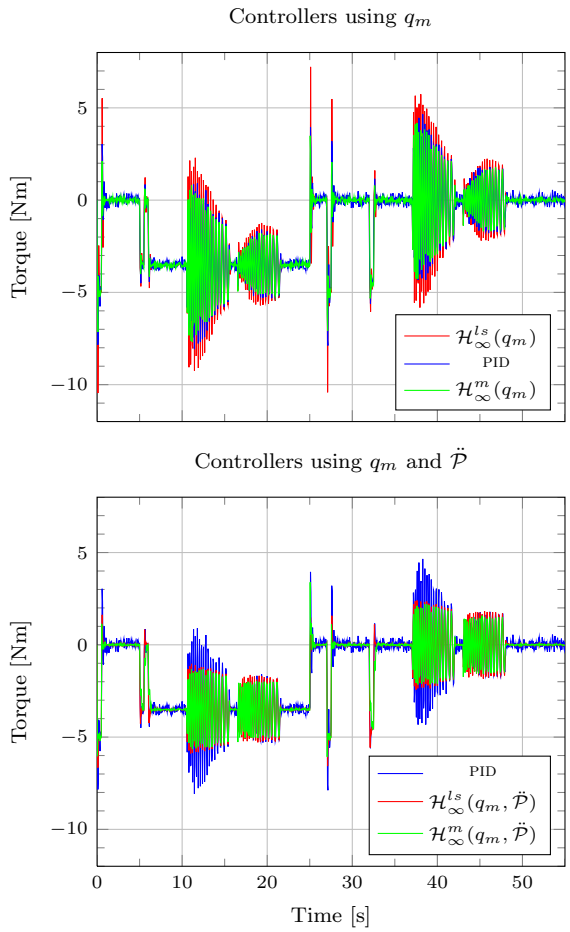

Fig. 5. Applied motor torque from the five controllers. The top graph shows the controllers using only q_m. The bottom graph shows the PID and the controllers using q_m and $\ddot{\mathcal{P}}$.

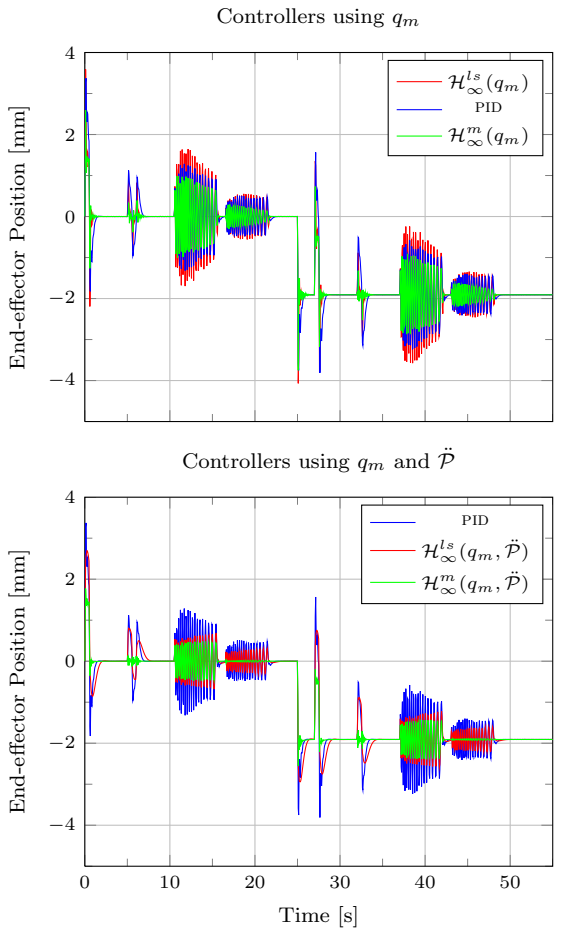

Fig. 6. Simulated end-effector position for the five controllers. The top graph shows the controllers using only q_m. The bottom graph shows the PID and the controllers using q_m and $\ddot{\mathcal{P}}$.

Table 1. Performance index for the five controllers, where lower value is better.

PID	$\mathcal{H}_\infty^{ls}(q_m)$	$\mathcal{H}_\infty^{ls}(q_m, \ddot{\mathcal{P}})$	$\mathcal{H}_\infty^{m}(q_m)$	$\mathcal{H}_\infty^{m}(q_m, \ddot{\mathcal{P}})$
55.7	55.4	45.8	42.4	28.8

controller in state space form requires $O(n_x^2)$ operations to calculate the control signal, where n_x is the dimension of the state vector in the controller.

The low order controllers are here obtained using the MATLAB-function `hinfstruct`, which is included in Robust Control Toolbox and it is based on techniques from Apkarian and Noll [2006].

To find controllers with low orders using `hinfstruct` requires a model description, including the weights, in the form of (1). This structure is already used for the controllers $\mathcal{H}_\infty^{m}(q_m)$ and $\mathcal{H}_\infty^{m}(q_m, \ddot{\mathcal{P}})$, hence it is straightforward to synthesis low order controllers using the weights presented in Sections 4.2.3 and 4.2.4. For the loop shaping design method, the structure in Figure 1(b) can be rewritten in the form of (1) including the weights $W_1(s)$ and $W_2(s)$, explained in e.g. Zhou et al. [1996]. Using the rewritten structure, the low order controllers based on $\mathcal{H}_\infty^{ls}(q_m)$ and $\mathcal{H}_\infty^{ls}(q_m, \ddot{\mathcal{P}})$ can be obtained using the weights from Sections 4.2.1 and 4.2.2.

Table 2 shows the lowest order for the respective controllers, that can be achieved without changing the closed-loop performance too much. The table also shows the performance index obtained when the controllers are used in the simulation environment. The orders can be reduced by a factor of two to three but the performance of the reduced order controllers is worse than the full order controllers. Since the controller based on loop shaping with only q_m as measurement has the same performance for the full order controller as the PID controller, the low order controller gives a worse performance than the PID controller. The other full order controllers are much better than the PID controller and afford to get a reduced performance for the low order controllers without getting worse than the PID controller.

Finally, note that the controllers only represents local minima solutions, hence rerunning `hinfstruct` with other initial values can give a better, or worse, controller. To handle this, several initial values have been used in `hinfstruct`.

7. CONCLUSIONS AND FUTURE WORK

Four different $\mathcal{H}_\infty$ controllers for a flexible joint of an industrial manipulator are designed using mixed-$\mathcal{H}_\infty$ controller design and the loop shaping method. The model, on which the controllers are based, is a four-mass model.

Table 2. Lowest order of the controllers obtained using `hinfstruct`, with the order before reduction in brackets. The corresponding performance index from simulations is also shown.

	$\mathcal{H}_\infty^{ls}(q_m)$	$\mathcal{H}_\infty^{ls}(q_m, \ddot{\mathcal{P}})$	$\mathcal{H}_\infty^{m}(q_m)$	$\mathcal{H}_\infty^{m}(q_m, \ddot{\mathcal{P}})$
Order	5 (13)	4 (13)	5 (10)	7 (13)
Perf. ind.	60.8	49.4	48.3	40.8

As input, the controllers use either the motor angle only or both the motor angle and the acceleration of the end-effector. Tuning of the controllers requires understanding of both the synthesis method and how the system behaves. For example, the measurements for the mixed-$\mathcal{H}_\infty$ controller are first pre-filtered to give an estimate of the tool position. The weighting functions for the resulting SISO system, from input torque to the estimated tool position, are then chosen similar to the case where only the motor position is used.

The controllers are compared to a PID controller and it is shown that if only the motor angle is measured it is much better to use the mixed-$\mathcal{H}_\infty$ design method compared to loop shaping. If instead the end-effector acceleration is added then the performance is improved significantly for both methods. The steady state error for the end-effector position is unaffected since the accelerometer does not provide low frequency measurements. Using a low order controller synthesis method, it is possible to reduce the order of the controllers by a factor of two to three but at the same time a decrease in the performance index of 10–30 % can be observed.

Investigation of robustness for stability with respect to model errors is one of several future directions of research. The mixed-$\mathcal{H}_\infty$ method has an advantage compared to the loop shaping method since a model of the error is possible to incorporate in the augmented plant $P(s)$.

Another continuation is to investigate the improvement for other types of sensors. One possibility is to have an encoder measuring the position directly after the gearbox, i.e., q_{a1}. This will improve the stiffness of the system, although it will not eliminate the stationary error for the end-effector position. The ultimate solution is to measure the end-effector position, but for practical reasons this is in general not possible, instead the end-effector position can be estimated, as described in Axelsson [2012], Axelsson et al. [2012], Chen and Tomizuka [2013], and used in the feedback loop.

Extending the system to several joints giving a non-linear model, which has to be linearised in several points, is also a future problem to investigate. A controller, using the results from this paper, is designed in each point and for example gain scheduling can be used when the robot moves between different points.

REFERENCES

P. Apkarian and D. Noll. Nonsmooth $\mathcal{H}_\infty$ synthesis. *IEEE Trans. Automat. Contr.*, 51(1):71–86, January 2006.

P. Axelsson. Evaluation of six different sensor fusion methods for an industrial robot using experimental data. In *Proc. of the 10th Int. IFAC Symp. on Robot Contr.*, pages 126–132, Dubrovnik, Croatia, September 2012.

P. Axelsson, R. Karlsson, and M. Norrlöf. Bayesian state estimation of a flexible industrial robot. *Cont. Eng. Pract.*, 20(11):1220–1228, November 2012.

W. Chen and M. Tomizuka. Direct joint space state estimation in robots with multiple elastic joints. *IEEE/ASME Trans. Mechatron.*, 2013. DOI: 10.1109/TMECH.2013.2255308.

B. de Jager. The use of acceleration measurements to improve the tracking control of robots. In *Proc. of the IEEE Int. Conf. on Syst., Man, Cybern.*, pages 647–652, Le Touquet, France, October 1993.

E. Dumetz, J.-Y. Dieulot, P.-J. Barre, F. Colas, and T. Delplace. Control of an industrial robot using acceleration feedback. *J. of Intell. Robot. Sys.*, 46(2):111–128, 2006.

K. Glover and D. McFarlane. Robust stabilization of normalized coprime factor plant descriptions with $\mathcal{H}_\infty$-bounded uncertainty. *IEEE Trans. Automat. Contr.*, 34(8):821–830, August 1989.

K. Kosuge, M. Umetsu, and K. Furuta. Robust linearization and control of robot arm using acceleration feedback. In *Proc. of the IEEE Int. Conf. on Contr. and App.*, pages 161–165, Jerusalem, Israel, April 1989.

D. McFarlane and K. Glover. A loop shaping design procedure using $\mathcal{H}_\infty$ synthesis. *IEEE Trans. Automat. Contr.*, 37(6):759–769, June 1992.

S. Moberg, J. Öhr, and S. Gunnarsson. A benchmark problem for robust feedback control of a flexible manipulator. *IEEE Trans. Contr. Syst. Technol.*, 17(6):1398–1405, November 2009.

M. Readman and P. Bélanger. Acceleration feedback for flexible joint robots. In *Proc. of the 30th IEEE Conf. on Decision and Contr.*, pages 1385–1390, Brighton, England, December 1991.

M. Ruderman and T. Bertram. Modeling and observation of hysteresis lost motion in elastic robot joints. In *Proc. of the 10th Int. IFAC Symp. on Robot Contr.*, pages 13–18, Dubrovnik, Croatia, September 2012.

H. G. Sage, M. F. de Mathelin, G. Abba, J. A. Gangloff, and E. Ostertag. Nonlinear optimization of robust $\mathcal{H}_\infty$ controllers for industrial robot manipulators. In *Proc. of the IEEE Int. Conf. on Robot. and Automat.*, pages 2352–2357, Albuquerque, NM, USA, April 1997.

H. G. Sage, M. F. de Mathelin, and E. Ostertag. Robust control of robot manipulators: A survey. *Int. J. of Contr.*, 72(16):1498–1522, 1999.

S. Skogestad and I. Postletwaite. *Multivariable Feedback Control, Analysis and Design.* John Wiley & Sons, Chichester, West Sussex, England, second edition, 2005.

Y. D. Song, A. T. Alouani, and J. N. Anderson. Robust path tracking control of industrial robots: An $\mathcal{H}_\infty$ approach. In *Proc. of the IEEE Conf. on Contr. App.*, pages 25–30, Dayton, OH, USA, September 1992.

W. L. Stout and M. E. Sawan. Application of H-infinity theory to robot manipulator control. In *Proc. of the IEEE Conf. on Contr. App.*, pages 148–153, Dayton, OH, USA, September 1992.

`mixedHinfsyn`. MATLAB-software, 2013. Available at http://www.kuleuven.be/optec/software/mixedhinfsyn.

W. L. Xu and J. D. Han. Joint acceleration feedback control for robots: Analysis, sensing and experiments. *Robot. and Comp.-Integ. Manufac.*, 16(5):307–320, October 2000.

K. Zavari, G. Pipeleers, and J. Swevers. Multi-$\mathcal{H}_\infty$ controller design and illustration on an overhead crane. In *Proc. of the IEEE Conf. on Contr. App.. Part of the IEEE Multi-Conf. on Syst. and Contr.*, pages 670–674, Dubrovnik, Croatia, October 2012.

K. Zhou, J. C. Doyle, and K. Glover. *Robust and Optimal Control.* Prentice Hall Inc., Upper Saddle River, NJ, USA, 1996.